

## Interactions of ultraviolet-B radiation, mixing, and biological activity on photobleaching of natural chromophoric dissolved organic matter: A mesocosm study

Robert F. Whitehead, Stephen de Mora,<sup>1</sup> Serge Demers, and Michel Gosselin

Institut des sciences de la mer (ISMER), Université du Québec à Rimouski (UQAR), 310 allée des Ursulines, Rimouski, Québec G5L 3A1, Canada

Patrick Monfort

Laboratoire d'Hydrobiologie Marine et Continentale, Université Montpellier II-CNRS (UMR 5556), Case 093, F-34 095, Montpellier Cedex 05, France

Behzad Mostajir

Institut des sciences de la mer (ISMER), Université du Québec à Rimouski (UQAR), 310 allée des Ursulines, Rimouski, Québec G5L 3A1, Canada

### Abstract

A natural planktonic assemblage from the St. Lawrence Estuary was isolated in eight 1,500-liter outdoor mesocosms and subjected to combinations of fast or slow mixing regimes with natural solar radiation or natural solar radiation artificially enhanced with ultraviolet-B (UVB, 280–320 nm) radiation. The interdependent evolution of dissolved organic carbon (DOC), absorption by chromophoric dissolved organic matter (CDOM), chlorophyll *a* (Chl *a*), particulate organic carbon (POC), and bacterial abundance in the mesocosms was followed over a 10-d period. There was a net increase of Chl *a*, POC, and DOC in all systems over time; however, the slower mixing treatments had less accumulation than the systems with faster mixing. All systems displayed weak correlations of DOC with POC and Chl *a*. A significant effect of enhanced UVB radiation on concentrations of these bulk properties was not observed in any of the mesocosms. A strong correlation of CDOM absorbance loss (photobleaching) with absorbed radiation dose was observed in all treatments, with the fast mixing systems having larger absorbance losses and faster loss rates. Photobleaching was wavelength dependent, resulting in an increase in the spectral slope of CDOM absorption over time. Thus, although CDOM photobleaching may result in deeper penetration of light at all wavelengths, the ratios of UVB to ultraviolet-A (UVA) and photosynthetically active radiation (PAR) are reduced. The effect of enhanced UVB radiation was unexpected, with no proportional increases in CDOM photobleaching in the +UVB treatments. Comparisons of the different treatments indicate that interactions of biological activity, mixing, and the in situ light field can influence CDOM absorbance properties and/or photoreactivity and that there is a possible role for UVB in the production of CDOM.

Numerous recent reports indicate that dissolved organic matter (DOM) plays a more active role in the biogeochemical carbon cycle than had previously been thought and that its fate in the ocean is intimately related to photochemical processes in the upper water column (Miller 1994). Photo-

chemical degradation of DOM has been shown to generate a variety of products, including various reactive oxygen species (Blough and Zepp 1995), low molecular weight carbonyl compounds (Kieber et al. 1989, 1990; Mopper et al. 1991), carbon monoxide (Valentine and Zepp 1993), and carbon dioxide (Miller and Zepp 1995; Gao and Zepp 1998). The transformation of complex, high molecular weight components into smaller, more labile moieties may stimulate bacterial production and lead to increased remineralization of otherwise biologically inaccessible compounds (reviewed in Moran and Zepp 1997). On the other hand, photochemical reactions have also been proposed as one of the steps in the formation of marine humic substances from biologically labile fatty acids (Harvey et al. 1983; Kieber et al. 1997), and some fraction of plankton-derived DOM may be relatively resistant to ultraviolet (UV) degradation (Ridal and Moore 1993). These findings have given new insights into the cycling of DOM in the ocean and offer viable pathways to resolve the perplexing problem of what happens to apparently recalcitrant terrigenous DOM in the ocean (*see* Hedges et al. 1997).

The first step in a photochemical process in natural water bodies is the absorption of sunlight. The DOM fraction con-

<sup>1</sup> To whom correspondence should be addressed. Present address: International Atomic Energy Agency, Marine Environment Laboratory, 4 Quay Antoine 1er, BP 800, MC98012, Monaco (S.de.Mora@iaea.org).

### Acknowledgements

This work was supported by funds from NSERC of Canada, Fonds FCAR of Québec, and NATO collaborative grant CRG95139. R.F.W. received doctoral research scholarships from Fondation de l'UQAR and Groupe de recherche en environnement côtier. We thank Peter Lee, Daniel Martel, Dominic Bélanger, Claude Belzile, Louis Pageau, Diane Berubé, Sarah Doiron, Marie-Eve Garneau, and Jacques Coté for technical and logistical support. We thank Suzanne Roy for discussions of unpublished data. The constructive comments of Mary Ann Moran and two anonymous reviewers helped improve the manuscript. This work is in partial fulfillment of R.F.W.'s Ph.D. thesis requirements at UQAR and is a contribution to the research program of the Groupe de recherche en environnement côtier.

taining chromophores (CDOM) absorbs light at wavelengths in the solar spectrum and is implicated in most photochemical reactions in natural waters (Zafiriou et al. 1984). Although CDOM potentially contains a large number of different chemical compounds and structures, its absorption spectrum is generally a featureless, nearly exponential decay from UV into visible wavelengths (Green and Blough 1994). The strong absorption in the UV range has been of particular interest in relation to its ability to attenuate ultraviolet-B (UVB) radiation in natural waters (e.g., Williamson et al. 1996) and thus mitigate the potentially biologically damaging effects of increased UVB due to ozone depletion (recently reviewed in Booth et al. 1997). However, photochemical reactions following absorption can eventually lead to the degradation of DOM and destruction of the chromophores (Zepp et al. 1995). This decrease in CDOM absorptivity, often termed photobleaching, may limit the UVB protective capacity of CDOM for organisms (Gao and Zepp 1998) and the extent of further photochemical reactions (Miller and Zepp 1995).

Previous studies investigating CDOM photobleaching have generally used filtered, natural waters or redissolved extracts of DOM irradiated by either sunlight or artificial light sources (Kouassi and Zika 1992; Morris and Hargreaves 1997). In addition, most studies have used optically thin solutions in small reaction vessels and thus are directly comparable to only the upper few centimeters of a natural water column. While useful in elucidating photochemical reactions and mechanisms, these studies are not strictly applicable to the prediction of in situ water column processes where autochthonous DOM from planktonic organisms (Gao and Zepp 1998), mixing (Doney et al. 1995), and changes in the underwater light field may influence photoreactions (Zepp and Cline 1977). The study presented here describes a mesocosm experiment where unaltered, natural seawater from the St. Lawrence Estuary with its intact planktonic assemblage ( $<202 \mu\text{m}$ ) was exposed to natural solar radiation and artificially UVB-enhanced solar radiation over a period of 10 d. Daily measurements of CDOM absorption coefficients, dissolved organic carbon (DOC) concentrations, incident and underwater irradiance, and indices of biological activity are used to evaluate the relationship between photochemical and biological processes in the determination of the optical properties of CDOM. One goal of this work was to determine whether a DOM pool that included autochthonously produced algal DOM would undergo absorbance photobleaching in a similar pattern to that seen in studies without biological input. Further goals were to evaluate the response of absorbance photobleaching to increased UVB and to different mixing regimes in the water column.

## Materials and methods

*Mesocosm setup*—In the late evening of 21 July 1997, ~25,000 liters of St. Lawrence Estuary seawater was pumped with a zooplankton pump from 2-m depth near the quay at Sainte-Anne-des-Monts, Québec, Canada (49°08'N, 66°29'W) into a thoroughly cleaned, stainless steel tanker truck. The truck was rinsed with copious quantities of sea-

water before the final filling. The seawater was delivered to the ISMER aquaculture station, Pointe-au-Père, Québec, Canada (48°51'N, 68°29'W), where it was transferred via a zooplankton pump into four 2.55-m high, 1.30-m diameter double-walled, stainless steel, outdoor tanks. Each tank was fitted with two open-top polyethylene bags to allow replication of experimental conditions within each tank and thus provided eight mesocosms of 2.25-m depth and 1,500-liter volume. To provide homogeneous starting conditions for the individual mesocosms, the water exiting the pump was initially filtered through a 202- $\mu\text{m}$  plankton net into a 100-liter tank fitted with eight tubes at the bottom that simultaneously drained by gravity into each of the mesocosms (Belzile et al. 1998).

Each mesocosm was mixed continuously using a system of 2.5-cm ID Tygon® tubing and a Teflon® coated Little Giant® pump (model 2-HD-HC). The pump intake was located 15 cm below the water surface, and the outflow was piped to the maximum depth of 2.25 m. Samples were drawn from a valve connected to a T in the outflow tubing. The entire pumping system for each mesocosm had been flushed with local seawater for a minimum of 300 h before the experiment began. Previous work (Belzile et al. 1998) had verified that the pumping system did not induce damage to planktonic cells. Water temperature within the mesocosms was controlled by circulating local seawater, 8–10°C, through the inner cavity of the double-walled tanks. Water removed from the mesocosm bags during the sampling was not replaced, but the water level was held constant in relation to the top of the tanks by adding water between the polyethylene bags and the tank walls after each sampling. No additional nutrients were added during the experiment, and the mesocosms were open to atmospheric exchange. Polyethylene covers were installed over the tops of the mesocosms during periods of rain and at night.

Four different combinations of light and mixing regimes were used for the experiment and will be referred to as follows: (1) NAT fast—natural ambient incident solar radiation and rapid turnover; (2) +UVB fast—ambient incident solar radiation plus added UVB radiation and fast turnover; (3) NAT slow—natural ambient incident solar radiation and slow turnover; and (4) +UVB slow—natural ambient incident solar radiation plus added UVB radiation and slow turnover. To simulate the effects of a reduced ozone layer, UV radiation was added to the ambient incident solar radiation by means of two Spectronics model XX15B ultraviolet lamps. The combined lamp output was a constant 111  $\mu\text{W cm}^{-2}$  in the 280–320-nm range and 86  $\mu\text{W cm}^{-2}$  in the 320–400-nm range (Belzile pers. comm.) with peak output at 313 nm (Fig. 1A). Cellulose acetate sheets (0.13 mm, aged 1 h before use and changed daily) were used to remove all lamp-emitted wavelengths shorter than 280 nm. The lamps were placed 40 cm above the water surface and were illuminated from 1000 to 1500 h each day. Wooden cutouts of the same dimensions as the lamps were placed over the natural light mesocosms to mimic any shading of the natural sunlight caused by the lamps. The lighting setup, except for the illumination period, was essentially the same as the low UVB (LUVB) regime described in Belzile et al. (1998), which presents a more complete discussion of the lamp spectra and

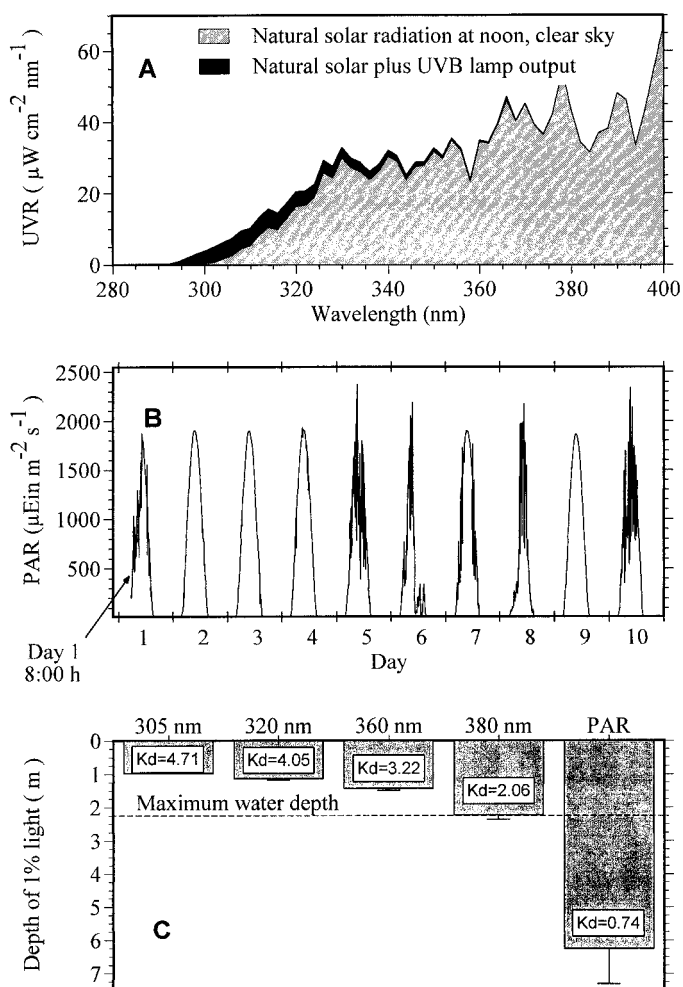


Fig. 1. (A) Noontime natural UV irradiance measured on a clear, sunny day. The output of the two UVB lamps was added to the natural spectrum to produce the enhanced UVB treatments. (B) Daily variations of incident PAR measured over the 10-d period of the experiment shown to illustrate the general meteorological conditions. (C) Apparent attenuation coefficients ( $K_d$ ,  $\text{m}^{-1}$ ) for 305, 320, 360, and 380 nm and PAR as derived from irradiance depth profiles in the mesocosms. The corresponding depth (m, +SD) of 1% near-surface irradiance ( $-0$  m) at each wavelength is indicated by the bars. The maximum depth of the mesocosms was 2.25 m.

their relationship to ambient light conditions. The two mixing regimes were controlled by varying the flow rates of the pumping systems using rheostats attached to the pump motors. The fast turnover regime had a flow rate that passed the entire volume of the mesocosm through the pump approximately every hour. The slow turnover rate passed the mesocosm volume through approximately every 3 h.

**Irradiance measurements**—Incident solar radiation was measured every 5 min using a Biospherical Instruments PUV-510 radiometer mounted in an unshaded area near the mesocosms. The PUV-510 uses cosine collectors to record downwelling irradiance of four UV wavelengths (nominally 305, 320, 340, and 380 nm) and an integrated, downwelling irradiance for photosynthetically active radiation (PAR, 400–

700 nm). The 305-nm channel was corrected according to the recommendations of Kirk et al. (1994). Irradiance measurements just below the water surface were taken regularly throughout the day with a Biospherical Instruments PUV-500 submersible radiometer equipped with depth and temperature sensors. The PUV-500 records the same wavelengths as the PUV-510. Vertical irradiance depth profiles were taken daily near 1300 h. Measurements were taken at  $\sim 2$ -cm depth intervals from just below the water surface to 1.6 m, the maximum depth allowed by the sensor configuration. In order to minimize the influence of clouds or shading from the mesocosm walls on the underwater measurements, profiles from three different positions in each mesocosm were taken. Apparent attenuation coefficients ( $K_d$ ,  $\text{m}^{-1}$ ) were calculated from Eq. 1 for each profile and the average was taken to represent the whole mesocosm:

$$K_{d\lambda} = \frac{\ln(E_{-0\lambda}/E_{z\lambda})}{\Delta z} \quad (1)$$

where  $z$  is depth in meters,  $E_{-0\lambda}$  and  $E_{z\lambda}$  are irradiance measured just below the surface and depth  $z$ , respectively.  $K_d$  values for the UV wavelengths where irradiance was not measured were estimated from the equation of the least-squares regression curve of a two-parameter exponential decay fitted to the measured data ( $r > 0.99$ ). Although  $K_d$  is often treated as an inherent optical property, it is sensitive to the geometric conditions of the light field (Kirk 1994). In the current paper, this discrepancy was corrected for by dividing  $K_d$ , as determined above, by Gordon's (1989) correction factor ( $D_{0\lambda}$ ), which is calculated from the direct fraction of global irradiance and the cosine of the angle of underwater refracted light. As these factors are dependent on sky conditions and solar zenith angles (SZA), the average  $D_{0\lambda}$  value of 1.19 for the St. Lawrence system from Kuhn et al. (1999) was used. Their average value was calculated from a range of solar zenith angles and sky conditions. It is worth noting that the average  $D_{0\lambda}$  is nearly identical to that which would be calculated (1.197) using 100% diffuse light. In the case of 100% diffuse light, SZA no longer influences the correction factor magnitude. Owing to shading from the mesocosm setup, it is reasonable to assume that the mesocosm water columns received a larger percentage of diffuse radiation than open waters in the St. Lawrence. Other irradiance calculations were made in the same manner as those reported in Belzile et al. (1998) with further refinements to models by the incorporation of irradiance data from the present experiment.

**Sampling and analytical methods**—Beginning on 22 July 1997, surface samples (15-cm depth) were collected daily between 0800 and 0900 h and immediately carried to the nearby laboratories. All containers were thoroughly rinsed with water from their respective mesocosm before the final sample was taken. Samples for DOC and absorbance measurements were collected in acid-soaked (2N HCl) 1-liter Nalgene® bottles. These samples were immediately filtered through precombusted (450°C for 24 h) Whatman® GF/F filters using gentle vacuum and stored in amber, glass bottles with teflon-lined caps at 4°C in the dark until analysis. DOC samples were acidified to  $\sim \text{pH } 2$  with 50% w/w  $\text{H}_3\text{PO}_4$  (5

$\mu\text{L mL}^{-1}$ ). All glassware and glass storage bottles were acid soaked, rinsed 5 times with  $>18 \Omega\text{m}$  resistivity, NANOpure-UV water (referred to as NANOpure water for simplicity) and subsequently combusted at  $450^\circ\text{C}$  for 24 h.

DOC was measured using the high temperature catalytic oxidation (HTCO) method with NDIR detection on a Shimadzu TOC-5000A carbon analyzer following the precautions of Benner and Strom (1993). Potassium diphthalate dissolved in NANOpure water was used as the carbon standard and NANOpure water as the blank. Triplicate injections of each sample were made and provided coefficients of variation of  $<2\%$ . Samples for absorbance were warmed to room temperature, gently sonicated, and filtered through  $0.2\text{-}\mu\text{m}$ , acid-washed Gelman Supor polysulfonone filters. Absorbance scans from 270 to 800 nm, 1-nm slit width, were made using 10-cm Suprasil cuvettes on a Perkin-Elmer Lambda 12 dual-beam spectrophotometer connected to a microcomputer equipped with UV-WINLAB software. Prefiltered ( $0.2 \mu\text{m}$ ) NANOpure water was used in the reference cell, and an autozero was run after every fifth sample. Absorbance measurements at each wavelength ( $\lambda$ ) were baseline corrected by subtracting the absorbance at 700 nm multiplied by  $\lambda/700$  (Bricaud et al. 1981). This wavelength-dependent approach was adopted, as opposed to the constant offset method suggested by Green and Blough (1994), owing to slight variations in the 700–800-nm readings, which suggested that differences may not have been solely due to refractive index differences between the NANOpure reference and the sample. Nevertheless, the required corrections were minor ( $0.0008 \pm 0.0004$  absorbance units,  $n = 34,400$ ). CDOM absorption coefficients ( $a_{\text{CDOM}\lambda}$ ,  $\text{m}^{-1}$ ) at each wavelength ( $\lambda$ ) were calculated according to Kirk (1994):

$$a_{\text{CDOM}\lambda} = 2.303A_\lambda/l \quad (2)$$

where  $A_\lambda$  is the corrected spectrophotometer absorbance reading at wavelength  $\lambda$  and  $l$  is the optical pathlength in meters. An average standard deviation (SD) of  $\pm 0.02 \text{ m}^{-1}$  for  $a_{\text{CDOM}\lambda}$  was estimated from repeated replicate measurements of the same sample. A conservative detection limit of  $0.046 \text{ m}^{-1}$ , corresponding to 0.002 absorbance units on the spectrophotometer, was estimated from repeated scans of NANOpure water processed as a sample. Although the detection limit corresponds to wavelengths in the range of 495 to 550 nm for the mesocosm samples, the actual scans were relatively noise free and reproducible throughout the PAR wavelengths.

All other measurements were made from subsamples of a 20-liter sample collected in dark, acid-soaked polyethylene carboys. Chlorophyll *a* (Chl *a*) concentration was determined fluorometrically using a R010 Turner Designs fluorometer from subsamples filtered onto GF/F filters and subsequently extracted for 24 h in 90% acetone at  $4^\circ\text{C}$  (Parsons et al. 1984). Samples for particulate organic carbon (POC) were collected on precombusted GF/F filters ( $450^\circ\text{C}$  for 24 h) and stored at  $-20^\circ\text{C}$  until analysis. Inorganic carbon was removed by acidification and the filters were subsequently dried at  $60^\circ\text{C}$  for 24 h. POC was analyzed on a Perkin-Elmer 2400 CHN elemental analyzer using acetonilide as the standard. Subsamples for bacterial abundance were fixed with formaldehyde (3.7% final concentration) and stored at  $4^\circ\text{C}$ .

Afterward, cells were stained with 4', 6-diamidino-2-phenylindole (DAPI) (Porter and Feig 1980) and counted using an ACR 1400SP flow cytometer following the method of Monfort and Baleux (1992).

Statistical analyses were performed using the means obtained from the two replicates in each of the mesocosm treatments. SigmaStat software was used for statistical tests. Trends in the data were fit to curves using least-squares regressions with significance evaluated at the  $p < 0.05$  level. Significant differences in trends between treatments were determined using the 95% confidence intervals of the regression coefficients. Other correlations were performed using Spearman rank order. Significance was evaluated at the  $p < 0.05$  level. For data with no obvious trends, two-way ANOVA (light and mixing as grouping variables) using all available data points was performed. Comparisons of individual time points could not be carried out with ANOVA due to the lack of sufficient replicates.

## Results

*Incident and underwater irradiance*—During the 10 d of the experiment, meteorological conditions were generally favorable with 5 d (days 2, 3, 4, 7, and 9) of clear-sky conditions, 4 d (days 1, 5, 8, and 10) of intermittent cloudiness, and 1 d (day 6) of heavy overcast with rain (Fig. 1B). Owing to shading from the mesocosm setup, the radiation actually entering the water columns was less than the incident radiation. For example, at noon under clear-sky or cloudy conditions, PAR just under the water surface was approximately 62 or 39% of the incident irradiance, respectively. Previous work with the same mesocosms (Belzile et al. 1998) and measurements made during the present work showed that the irradiance just below the water surface ( $E_{-0\text{m}}$ ) could be modeled from the measured incident irradiance ( $E_0$ ), sky conditions, time of day, and lamp outputs. The calculated, daily integrated, radiation doses received just below the water surface for the two light treatments are given in Table 1.

Vertical attenuation of downwelling irradiance was in part controlled by the mesocosm configurations. The  $K_d$  values, as determined from Eq. 1, did not vary significantly (ANOVA  $p > 0.05$ ) among mesocosms during the experiment (Fig. 1C). These measurements revealed a stronger attenuation of PAR,  $K_{d\text{PAR}} = 0.737 \text{ m}^{-1}$ , than occurs in the open waters of St. Lawrence Estuary. Although  $K_{d\text{PAR}}$  was not measured at the initial sampling site, literature reports of  $K_{d\text{PAR}}$  in nearby waters ranged from 0.29 to  $0.53 \text{ m}^{-1}$  (Levasseur et al. 1984) and from 0.155 to  $0.242 \text{ m}^{-1}$  in the Gulf of St. Lawrence (Larouche 1998). These values equate to a 1% light depth ranging from 8.7 to 29.7 m as compared to 6.25 m in the mesocosms. Attenuation of UV wavelengths in the mesocosms was also greater than that in the St. Lawrence Estuary. Kuhn et al. (1999) reported  $K_{d310\text{nm}}$  ranging from 0.7 to  $4.5 \text{ m}^{-1}$  in the St. Lawrence Gulf and Estuary during summer and autumn. At their station closest to our sampling site, the  $K_{d310\text{nm}}$  was  $3.29 \text{ m}^{-1}$ , which is considerably less than the  $4.48 \text{ m}^{-1}$  in the mesocosms. In comparison with other natural water bodies, however, light attenuation in the mesocosms was not outside the range of turbid coastal

Table 1. Daily integrated radiation dose received just below the water surface.

Day	305 nm*		320 nm*		340 nm*		380 nm*		PAR†	
	NAT	+UVB	NAT	+UVB	NAT	+UVB	NAT	+UVB	NAT	+UVB
1	0.216	1.071	2.41	3.17	4.43	4.74	6.20	6.22	18.18	18.18
2	0.312	1.166	3.31	4.07	6.16	6.47	9.13	9.14	28.47	28.47
3	0.325	1.801	3.31	4.07	6.12	6.43	9.03	9.04	28.34	28.34
4	0.359	1.213	3.35	4.11	6.09	6.41	8.95	8.96	28.39	28.39
5	0.283	1.138	2.71	3.46	4.90	5.22	7.02	7.03	21.41	21.41
6	0.182	1.037	1.70	2.46	3.22	3.53	4.55	4.56	13.66	13.66
7	0.359	1.214	3.22	3.98	5.81	6.13	8.54	8.55	26.75	26.75
8	0.178	1.033	2.06	2.82	3.90	4.22	5.58	5.59	16.62	16.62
9	0.296	1.151	3.21	3.96	5.97	6.29	8.80	8.82	27.76	27.76
10	0.211	1.065	2.40	3.16	4.43	4.75	6.26	6.27	18.58	18.58
Total	2.721	11.88	27.68	35.26	51.03	54.19	74.06	74.18	228.2	228.2

\* UV measurements are in  $\text{kJ m}^{-2}$ .

† PAR measurements are in  $\text{Ein m}^{-2}$ .

areas and areas with high terrestrial DOM contributions (*see* Kirk 1994).

**Biological activity**—Although there are numerous possibilities for the estimation of biological activity in the mesocosms, for the purpose of this work Chl *a* concentration was used as a proxy for phytoplanktonic biomass and POC as a proxy for planktonic biomass and overall productivity. The two mixing treatments had a discernible effect on biological activity within the mesocosms. As shown in Fig. 2, the initial variables were virtually identical for all the treatments; however, by day 10 the fast mixing systems exhibited higher concentrations of both Chl *a* and POC. From day 1 to day 5, both mixing systems showed steady increases in Chl *a* from  $0.8 \mu\text{g L}^{-1}$  to  $\sim 3.0 \mu\text{g L}^{-1}$ . From day 7 on, the fast systems continued to increase, reaching  $\sim 6.0 \mu\text{g L}^{-1}$  on day 10 (Fig. 2A), whereas the slow systems leveled off from day 7 to day 10 with final concentrations  $\sim 4.0 \mu\text{g L}^{-1}$  (Fig. 2E). In contrast to the mixing influence, enhanced UVB radiation did not alter the accumulation of Chl *a* in either mixing treatment. POC was positively correlated with Chl *a* concentration in both mixing and light treatments throughout the experiment with an *r* of 0.952, 0.867, 0.758, and 0.705 in the NAT fast, +UVB fast, NAT slow, and +UVB slow treatments, respectively (Spearman rank order,  $p < 0.05$ ). The increase in POC was somewhat slower than Chl *a* concentration, resulting in a 3.5-fold increase in the Chl *a*:POC ratio in the fast systems and a 2.5-fold increase in the slow systems with no apparent UVB-induced differences. Bacterial abundance appeared to be uncoupled from the increases in Chl *a* and POC concentrations. Bacterial abundance tripled from  $\sim 1 \times 10^6$  to  $3 \times 10^6$  cells  $\text{mL}^{-1}$  from day 1 to day 5 in the fast systems (Fig. 2C). During this same period, bacterial abundance in the slow systems doubled from  $\sim 1 \times 10^6$  to  $2 \times 10^6$  cells  $\text{mL}^{-1}$  (Fig. 2G). Thereafter, a sharp drop was seen on days 6, 7, and 8 in both mixing systems, with abundances below those measured on day 1. A slight recovery to  $\sim 1 \times 10^6$  cells  $\text{mL}^{-1}$  was seen in the fast systems on days 9 and 10. As with Chl *a* and POC concentrations, bacterial abundance was consistently higher in the fast systems as compared to the slow and no UVB effect was discernible within either mixing treatment.

**DOC concentrations**—Concentrations of DOC measured on day 1 (Fig. 2D,H) were similar to those previously reported for nearby stations in the St. Lawrence Estuary (Nieke et al. 1997; Larouche 1998; Kuhn et al. 1999) and other coastal waters of eastern North America (Vodacek et al. 1997). From day 1 through day 5, there was a general downward trend in DOC in the slow treatments, whereas the trend in the fast systems was fairly flat (Fig. 2D,H). On day 7, DOC concentrations in the slow systems started to recover and began increasing in the fast systems as well. In the fast systems, final DOC concentrations exceeded initial concentrations by about  $20 \mu\text{M C}$ . The recovery was not as strong in the slow turnover systems, as final values were approximately equal to day 1. The changes in DOC during the latter part of the experiment were similar to changes in Chl *a* and POC concentrations. DOC concentration in the fast systems were weakly but significantly correlated ( $p < 0.05$ ) with both Chl *a* ( $r = 0.58$ ) and POC ( $r = 0.67$ ) concentrations over the whole experimental period. However, correlations of DOC with POC or Chl *a* concentration were not significant in the slow systems when considering the entire 10 d of the experiment. In addition, there were no significant differences due to UVB within either mixing treatment for DOC. Bacterial abundance showed weak, negative correlation with DOC in all treatments (*r* ranging from  $-0.37$  to  $-0.76$ ), which were significant in both +UVB treatments ( $p < 0.05$ ). The increase in DOC at the end of the experiment suggests that bacteria were not carbon limited and possibly indicates that other controls on bacterial activity such as grazing, inorganic nutrient limitation, or viral lysis were more important than carbon availability within the mesocosms. On the other hand, phototransformation of labile DOM may have also been a factor in reducing substrate bioavailability (Obernosterer et al. 1999). The uncoupling of primary production and bacterial abundance during the final 4 d of the experiment was probably responsible for the observed DOC accumulation during this period.

**CDOM absorption coefficients**—CDOM absorption coefficients ( $a_{\text{CDOM}}$ ) measured on day 1 agreed well with those measured previously (July 1990) in St. Lawrence Estuary waters at comparable salinity (Nieke et al. 1997). For ex-

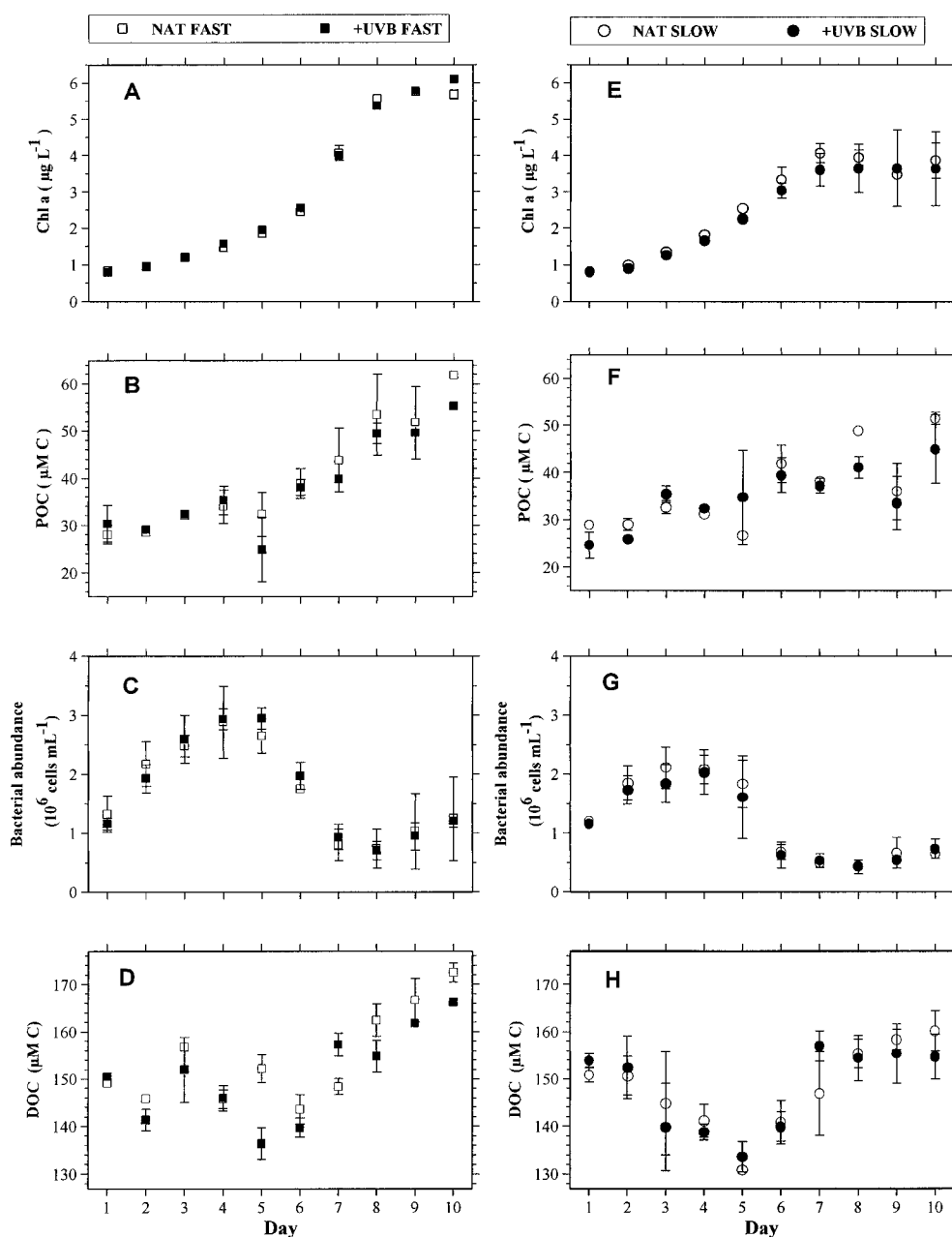


Fig. 2. Daily variations in Chl *a* concentration, POC concentration, bacterial abundance, and DOC concentration for the two mixing treatments. Left-hand side (A, B, C, D) are the two light treatments in the fast turnover systems and the right-hand side (E, F, G, H) are the two light treatments in the slow turnover systems. Error bars show the range of the observations.

ample, on day 1 the average  $a_{\text{CDOM}}$  at 365 nm was  $0.98 \text{ m}^{-1}$  in the mesocosms, as compared to  $1.0\text{--}1.2 \text{ m}^{-1}$  for waters from 2 m in the St. Lawrence (Nieke et al. 1997). However, the initial values did not remain constant over the course of the experiment, with CDOM absorption coefficients showing clear decreases across the entire absorption spectrum in all treatments (Fig. 3). As previously reported in other photobleaching experiments (Kieber et al. 1990; Kouassi and Zika 1992), the largest absolute decreases in absorbance occurred in the UVB range (Table 2). However, due to much lower initial absorbances, the greatest losses as a percentage of initial values were seen at longer wavelengths. It should be

noted that the PAR loss values for  $a_{\text{CDOM}}$  in Table 2 include wavelengths from 400 to 700 nm, whereas the detection limit for  $a_{\text{CDOM}}$  generally corresponded to  $\sim 495 \text{ nm}$ . Because calculations using the range from 400 to 495 nm yield the same trends in both absolute and percentage losses, the average of the entire PAR range is presented to maintain consistency with the irradiance measurements.

*Kinetics of photobleaching*—Previous studies of CDOM absorbance photobleaching have shown that the process generally follows pseudo first-order kinetics when using optically thin samples (Kouassi and Zika 1992; Gao and Zepp

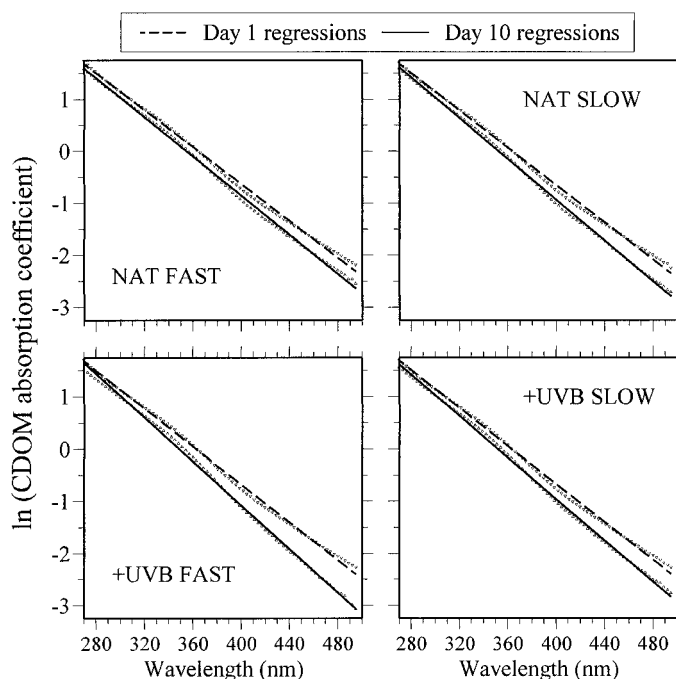


Fig. 3. Natural logarithms of the CDOM absorption coefficients for the different mesocosm treatments as measured on day 1 and day 10 versus wavelengths. Small points are the actual values, and lines are the fitted least-squares regressions ( $r > 0.99$ ). Ninety-five percent confidence intervals fall within the width of the regression lines shown.

1998). On the other hand, when the system under consideration is optically thick, the kinetics of photochemical reactions become zero-order (Miller 1998). Light absorbance in the mesocosm water columns exceeded 99% for most UV wavelengths and was  $\sim 81\%$  for PAR. CDOM absorbance contributed an average of 49% of the total attenuation in the UV region and 14% in the PAR region. Therefore, the optically thick nature of the mesocosm water columns would tend to produce zero-order kinetics. Exposure to a constant light source would thereby yield linear decreases of CDOM absorbance due to photochemical reactions with time. However, due to differences in light treatments and the variations in incident solar radiation, the mesocosm data cannot be compared on a timescale. As such, the measured UV irradiance data was converted from  $\mu\text{W cm}^{-2} \text{nm}^{-1}$  into Einsteins ( $\text{Ein cm}^{-2} \text{nm}^{-1} \text{s}^{-1}$ ) according to the equation of Zepp

and Cline (1977) and then used to calculate the photon flux,  $E_{-0m}$ , just below the water surface. PAR, in  $\mu\text{Ein m}^{-2} \text{s}^{-1}$ , was measured directly as the integrated 400–700-nm band by the PUV 500. Incident irradiance measurements were taken every 5 min and were integrated over time to give daily and cumulative radiation doses. The UV photons added by the lamps were calculated from the lamp spectral characteristics, the measured increases in UV just below the water surface, and the period of lamp illumination. These values were added to  $E_{-0m}$  to provide the +UVB treatment photon fluxes. As a first approximation for the entire ultraviolet-A (UVA) and UVB spectrums, the daily integrated  $E_{-0m}$  values at 305, 320, 340, and 380 nm were fit to a sigmoidal curve forced to zero at 290 nm. The shortest incident wavelength measured at solar noon, shortly after the experiment, with an Optronics Laboratories OL 754 scanning spectrophotometer was 292 nm (1-nm resolution). Kuhn et al. (1999) reported the shortest wavelength measured just below the surface in the St. Lawrence was  $\geq 294$  nm. Their measurement was taken a month earlier on 15 June 1997, i.e., closer to summer solstice, at the same approximate latitude as the mesocosm location and with the same type of instrumentation. Comparisons with noontime full UV spectrum from the OL 754 indicated that this method could reproduce the integrated total UV or UVA irradiance within  $\pm 5\%$  and integrated total UVB within  $\pm 10\%$  with greatest uncertainty below 305 nm. Although values from the curves were used for interpolation, the actual measured irradiances for 305, 320, 340, and 380 nm were used in all rate calculations. As with the light data, the actual  $K_d$  values derived from irradiance data were used where available. The rate of photon absorbance by CDOM, ( $I_{a\lambda}$ ), was estimated from Eq. 3 (Miller 1998):

$$I_{a\lambda} = I_{-0\lambda}(1 - e^{-K_{d\lambda}l})F_{\lambda} \frac{\text{Area}}{V} \quad (3)$$

where  $I_{-0\lambda}$  is integrated downwelling irradiance just below the surface in  $\text{Ein cm}^{-2} \text{nm}^{-1} \text{d}^{-1}$ , the term in parentheses represents attenuation by the system over a pathlength of  $l$ ,  $F_{\lambda}$  is the fraction of light absorbed by CDOM determined from the ratio of  $a_{\text{CDOM}\lambda} : K_{d\lambda}$ , Area is the area of the light beam in  $\text{cm}^2$ , and  $V$  is the volume of the solution in  $\text{dm}^3$ . The irradiation geometry for all treatments is assumed to be equal with uniform light distributed over the surface area of the mesocosms. Because  $K_d$  was corrected for light geometry, the maximum depth of the mesocosms (2.25 m) was

Table 2. Average absolute daily  $a_{\text{CDOM}}$  loss (day, minus day<sub>+1</sub>) over the 10-d experimental period and average loss as a percentage of initial day, CDOM absorbance at selected wavelengths.

	305 nm		320 nm		340 nm		380 nm		PAR*	
	Loss ( $\text{m}^{-1} \text{d}^{-1}$ )	%	Loss ( $\text{m}^{-1} \text{d}^{-1}$ )	%	Loss ( $\text{m}^{-1} \text{d}^{-1}$ )	%	Loss ( $\text{m}^{-1} \text{d}^{-1}$ )	%	Loss ( $\text{m}^{-1} \text{d}^{-1}$ )	%
NAT fast	0.044	1.52	0.040	1.76	0.033	2.03	0.020	2.75	0.005	4.64
+UVB fast	0.041	1.46	0.036	1.64	0.030	1.92	0.019	2.75	0.005	4.95
NAT slow	0.033	1.15	0.030	1.35	0.027	1.69	0.015	2.15	0.004	3.82
+UVB slow	0.035	1.24	0.030	1.34	0.025	1.60	0.016	2.23	0.004	3.64

\* PAR loss was calculated from the average  $a_{\text{CDOM}}$  over the interval 400–700 nm.

used as the average pathlength of the diffuse underwater light.

Calculated CDOM absorbance rates may underestimate actual rates because downwelling irradiance was used instead of scalar irradiance ( $E_0$ ). However, because the ratio  $K_0:K_d$  varies only between 1.01 and 1.06, measured  $K_d$  also reasonably predicts attenuation of scalar irradiance (Kirk 1994). The exact ratio of  $E_0:E_d$  is a function of the ratio of the scattering to absorption coefficients, but is  $<1.8$  for most coastal waters (Kirk 1994). In the present study, the data required to quantify scattering in the mesocosms are not available. However, an estimate can be made as to whether or not scattering changed over time. As  $K_d$  is a manifestation of all attenuation processes (i.e., reflection, absorption, and scattering), the ratio of total absorption to  $K_d$  should remain constant if scattering remains constant. In the absence of absorbing particles, absorption processes can be defined as the sum of  $a_{\text{CDOM}}$  + absorption due to water + absorption due to plankton (Baker and Smith 1982). By use of the bio-optical predictive model of Baker and Smith (1982) in conjunction with the measured daily Chl *a* concentration in the mesocosms, the absorption coefficients of pure water (Kirk 1994) and the daily mesocosm  $a_{\text{CDOM}}$  measurements, the ratio of total absorption to  $K_d$  in the mesocosms varied by less than 4% during the experiment. This is within the estimated 5% error for the Baker and Smith model. Thus, the ratio of scattering to absorption, and consequently the ratio of  $E_0$  to  $E_d$ , appeared relatively constant. On the other hand, the same processes that maintained stable  $K_d$  values during the experiment, i.e., the concurrent decreases in  $a_{\text{CDOM}}$  and the increases in Chl *a* concentration, resulted in decreasing  $F$  ratios. However, the decreases in  $F$  ratios were not significantly different among the treatments. To account for these changes,  $F_\lambda$  for a given day,  $t$ , was calculated using the average  $a_{\text{CDOM}}$  of day  $t$  and day  $t+1$ .

Zero-order rate constants were calculated from the slopes of the least-squares linear regression fits of  $a_{\text{CDOM}}$  versus cumulative  $E_{\text{in}}$  absorbed. In effect, the slopes with units of  $a_{\text{CDOM}}$  ( $E_{\text{in}}$  absorbed) $^{-1}$  approximate the apparent quantum yields for photobleaching in the mesocosms. The term apparent quantum yield is used cautiously here to denote the lack of a molar basis for  $a_{\text{CDOM}}$  and the probable interactions of light from different wavelengths. In the first instance,  $a_{\text{CDOM}}$  was plotted against the cumulative number of  $E_{\text{in}}$  absorbed at that particular  $\lambda$ . For example, daily values of  $a_{305\text{nm}}$  were plotted as a function of the  $E_{\text{in}}$  absorbed at 305 nm (Fig. 4). Correlation coefficients averaged 0.973 for these least-squares regressions. Two striking features are shown by these rate constants. First, in the UVB regions, the NAT light treatments of both mixing systems have higher rate constants than do their respective +UVB treatments (significant difference at 305 and 320 nm in slow; at 305 in fast). Second, the slow systems have consistently lower rate constants than their respective light treatments in the fast systems (significant difference at 305 nm). Although these regression analyses had very good correlations, photobleaching was observed at wavelengths below 280 nm, where there were no incident photons measured. A similar result has also been reported in studies using monochromatic light (Kouassi and Zika 1992). This suggests that the rate of photobleaching

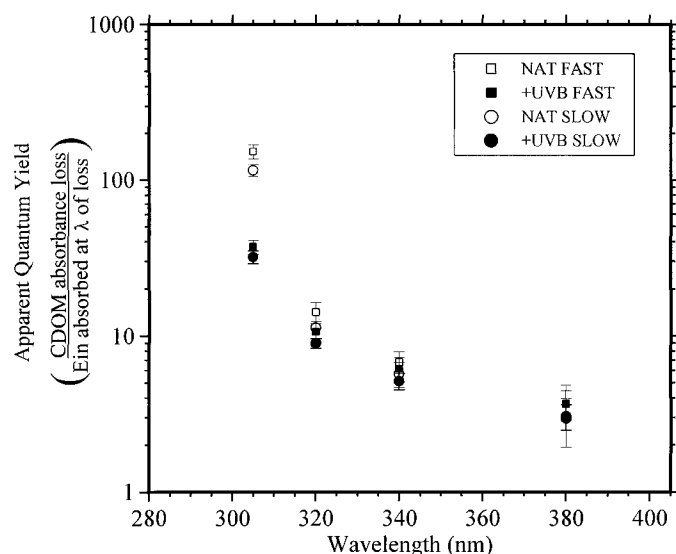


Fig. 4. Apparent quantum yields for photobleaching of CDOM absorbance. These yields are calculated as the slope of the least-squares regression lines of absorbance loss at a particular wavelength versus  $E_{\text{in}}$  absorbed at that same wavelength. Error bars are the 95% confidence intervals for the regression slope coefficients.

at any wavelength is not exclusively dependent on photons absorbed at that wavelength or that the destroyed chromophore absorbed over a range of wavelengths. As such, rate constants were also calculated for photobleaching versus total  $E_{\text{in}}$  absorbed 280–700 nm (Fig. 5A). In this case, which is approximately equal to one-half the  $d^{-1}$  rate with each day having an irradiance equal to the mean irradiance of the 10 d for the respective light treatments, the two mixing groups were also distinguishable from each other. The slow mixing systems showed generally lower rate constants than the fast systems, with significant differences between the NAT fast and NAT slow for  $\lambda < 305$  nm. Within the slow systems, the two light treatments had nearly identical photobleaching rates at all wavelengths except below 315 nm, where the +UVB system rates were slightly though not significantly higher. Within the fast systems, the rates for the two light treatments were not significantly different over the entire spectrum. These same groupings were also seen in plots of  $a_{\text{CDOM}}$  loss versus total UV and total UVA  $E_{\text{in}}$  absorbed, with the only significant differences being between NAT fast and NAT slow at  $\lambda < 310$  nm (Fig. 5B,C). The rates calculated versus total UVB absorbed (Fig. 5D), however, stand out from these trends. Here the treatments were more closely grouped in terms of light treatments rather than mixing with the two NAT treatments having faster rates than the +UVB treatments, which indicates that the added UVB radiation affected photobleaching rates, but in an unexpected manner (discussed later). In addition, the trend of faster photobleaching in the fast systems as compared to their respective slow light treatments demonstrates a mixing control.

*Spectral changes in CDOM absorption*—Least-squares regression fits of the natural logarithm of CDOM absorption coefficients versus wavelength were used to calculate a spec-

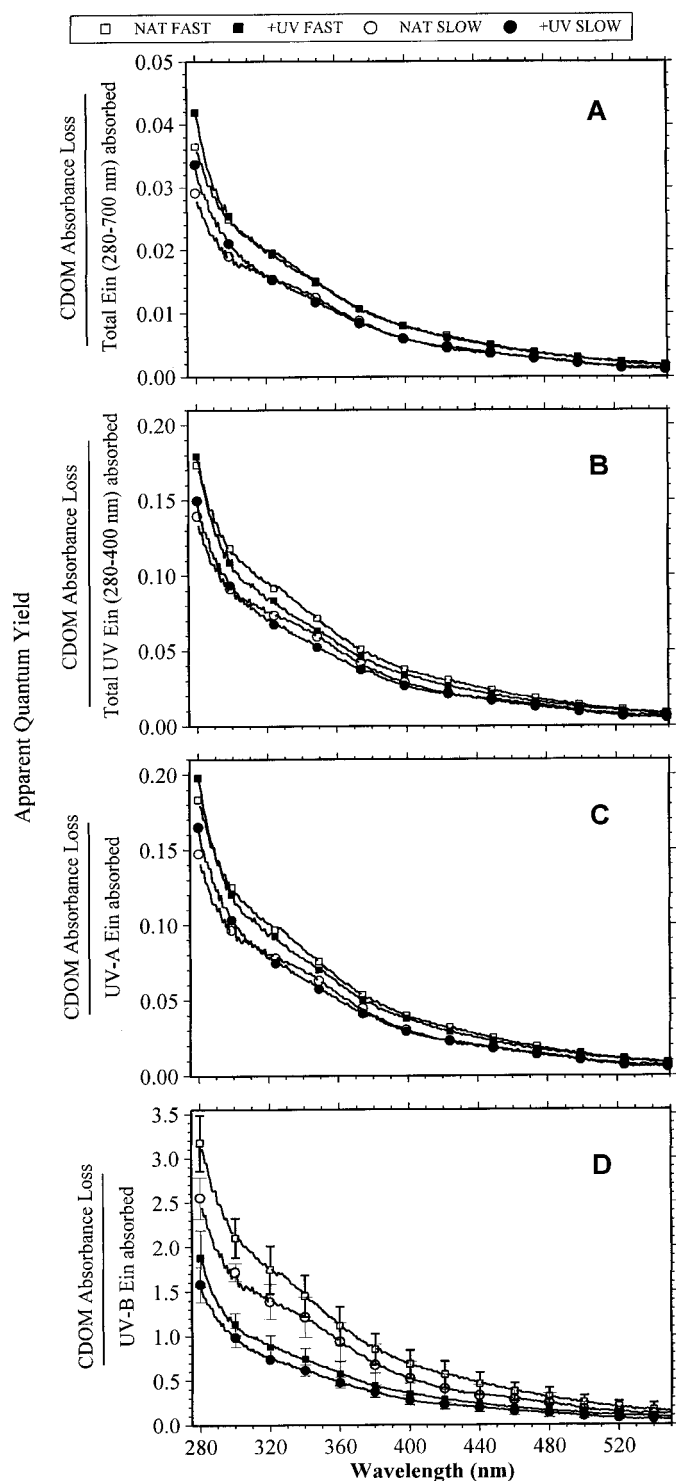


Fig. 5. Apparent quantum yields for photobleaching of CDOM absorbance calculated from least-squares regressions versus absorbed doses from different regions of the radiation spectrum. Apparent quantum yields calculated using (A) the cumulative absorbed dose from 280–700 nm, roughly equivalent to a one-half the rate of loss  $d^{-1}$  assuming each day received irradiance equal to the average of the respective light treatments; (B) the total cumulative UV (280–400 nm) absorbed dose; (C) the cumulative total UVA (320–400 nm) absorbed dose; and (D) the cumulative total UVB (280–320 nm) absorbed dose. Error bars are the 95% confidence intervals

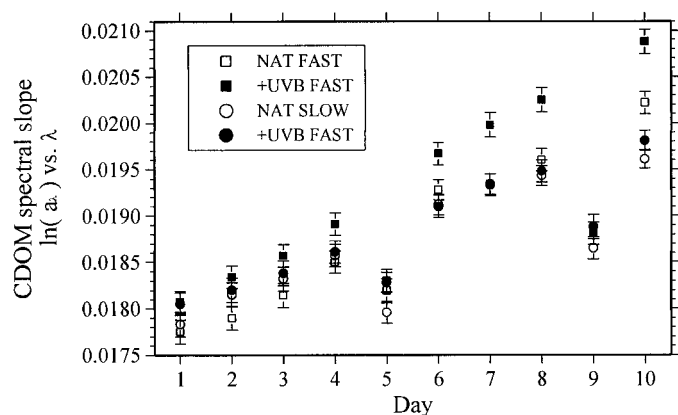


Fig. 6. Temporal variation in CDOM spectral slopes for the different mesocosm treatments. The slopes at each time point were calculated from  $\ln(a_{\text{CDOM}\lambda})$  versus  $\lambda$  over the wavelength interval 270–495 nm. Error bars are the 95% confidence intervals for the regression slope coefficients.

tral slope factor termed  $S$ . (Note that the slope of  $\ln a_{\text{CDOM}}$  versus wavelength is a negative value when wavelengths are used in ascending order on the  $x$  axis; however, most authors report  $S$  as the absolute value of this slope.) Previous studies have used  $S$  to compare the spectral characteristics of CDOM absorption or to extrapolate CDOM absorption coefficients for the entire spectrum from measurements at just one or a few wavelengths (Bricaud et al. 1981; Carder et al. 1989). However, the wavelength range over which the regression is performed has a substantial effect on the  $S$  obtained (Carder et al. 1989; Coble and Brophy 1994). For this reason, the regressions were determined over a fixed wavelength range from a lower limit of 270 nm. The upper wavelength limit of 495 nm was chosen to correspond to the lowest observed absorbance reading above the detection limit in any treatment or day and was found to occur in the NAT fast treatment on day 10. Therefore, reported  $S$  values are for  $\ln a_{\text{CDOM}\lambda}$  versus  $\lambda$  (270 to 495 nm) for all treatments and days (Fig. 6). Correlation coefficients for the regressions were  $>0.99$ .

The evolution of biochemical and photochemical processes during the experiment resulted in a change in the spectral characteristics of CDOM absorption. Figure 6 shows that there was a steepening in the spectral slopes for all treatments over the course of the 10 d. There was a slight difference in  $S$  with mixing treatments. Values for  $S$  in the fast systems increased 13.9% and 15.6% in the NAT and +UVB light treatments, respectively, whereas  $S$  in the slow systems increased 9.9% and 9.8% in the NAT and +UVB treatments, respectively. Although these differences were significant on day 10, the trends over time indicate that only the +UVB fast systems displayed a consistently different response.

←

for the regression slope coefficients. For sake of clarity, error bars are not included in (A), (B), or (C), see text for significant differences.

## Discussion

Owing to significant technical challenges, the majority of standing marine DOM pools remains ill defined in terms of chemical composition and structure (Hedges 1992), with DOM released from planktonic or bacterial activity being equally enigmatic. Although the DOM pool was not characterized in the present work, changes in DOC concentrations indicate active cycling of the DOM pools (Fig. 2D,H). Numerous previous studies have shown that releases of DOM through direct algal exudation, bacterial activity, and grazing are significant sources of marine DOM (Biddanda and Benner 1997; Stromm et al. 1997; Carlson et al. 1998), all of which were present in the mesocosms. Thus, in contrast to previous photochemical studies using filtered-water samples, DOM pools in the current study were evolving with time due not only to photochemical changes but also to compositional changes caused by biological production and consumption. Therefore, the results here represent the interdependent evolution of optical properties, photochemical processes, and biological activity in the mesocosms and may serve to bridge the gap between laboratory-based photochemical investigations and field observations. The concurrent biological activity may directly influence the optical properties of CDOM through production of compounds with different spectral absorbance characteristics or through preferential consumption of one part of the CDOM pool. At the same time, differing photoreactivities of algal-derived DOM may influence photochemical kinetics or possibly yield photoreactions not common to the initial mesocosm DOM, which in turn affects the CDOM optical properties.

Changes in  $S$  over the 10 d of the experiment may exemplify the processes that yield changes in CDOM properties with distance offshore. Since the mesocosms were filled with coastal waters from the St. Lawrence Estuary, the initial DOM pool was most likely terrestrially influenced. Photochemical degradation studies of filtered estuarine and freshwater samples have demonstrated that photobleaching in the absence of biota causes  $S$  to decrease (Miller 1994; Morris and Hargreaves 1997; Gao and Zepp 1998). In contrast, transect studies in coastal waters off the Eastern U.S. indicate that although CDOM absorption coefficients decrease with distance offshore,  $S$  values increase (Vodacek et al. 1997). A similar pattern of increasing  $S$  with increasing salinity has been noted in a wide range of coastal waters (Brown 1977; Blough et al. 1993; Nelson and Guarda 1995). This is perhaps not surprising given the isotopic and compositional differences of terrestrial and marine humic substances, which depict a change to a principally marine source for DOM with distance offshore (e.g., Guo and Santschi 1997). Carder et al. (1989) have suggested that changes in  $S$  may reflect differing proportions of humic and fulvic acids contained within CDOM with fulvic acids having higher  $S$  values than humic acids. Larger spectral slopes of marine CDOM are therefore possibly related to the higher percentage of fulvic acids in marine DOM (Malcolm 1990). Thus, the increase in  $S$  with salinity has been interpreted as both a mixing process involving terrestrial and marine end members (Blough et al. 1993; Nelson and Guarda 1995) and by photobleaching

in combination with changes in the source of CDOM (Gao and Zepp 1998). Although there were no changes in salinity, the results from the present experiment follow the transect data in that as  $a_{\text{CDOM}}$  was decreasing,  $S$  was steepening. Taken with the changes observed in DOC concentrations, the changes in  $S$  may reflect a move toward a more marine-influenced CDOM pool in the mesocosms either through photochemical or biological processes or a combination of the two.

Bacterial activity has been proposed to alter the molecular weight of DOM and cause subsequent increases in  $S$  (Pages and Gadel 1990; Vodacek et al. 1997). Other studies have shown that bacterial activity can transform low molecular weight (LMW) material into high molecular weight (HMW) material (Brophy and Carlson 1989). Nelson, et al. (1998) have suggested that CDOM production near the Bermuda Atlantic Time Series (BATS) station in the Sargasso Sea is controlled by microbial activity, but they did not report whether  $S$  was also influenced by microbial activity. Their  $S$  values fall at the upper end of most reported values, but it is noteworthy that they reported the highest values of  $S$  in the near-surface layer where photodegradation would be greatest. Likewise, Mopper et al. (1996) found that the spectral slopes of deep-water DOM from the Central Pacific were lower than surface samples, but whether this is a consistent trend is unknown. Vodacek et al. (1997) concluded that photodegradation and/or bacterial use of photo-oxidation products may be responsible for the shift in  $S$  during inshore offshore transects in the Atlantic Bight. Phototransformation of labile products into more refractory products has been shown (Keil and Kirchman 1994; Naganuma et al. 1996; Benner and Biddanda 1998), but information on accompanying changes in CDOM spectral characteristics is lacking. Both Vodacek et al. (1997) and Nelson et al. (1998) concluded that the direct in situ production of CDOM by phytoplankton was probably not involved due to the lack of strong covariance of Chl  $a$  concentration and CDOM. Moreover, other authors have noted the lack of strong correlations between Chl  $a$  concentration and CDOM (DeGrandpre et al. 1996; Rochelle-Newall et al. 1999), which suggests that if direct phytoplankton production is a significant source of CDOM, then Chl  $a$  and CDOM must be produced or degraded at different rates during and after a phytoplankton bloom (Carder et al. 1989). Nonetheless, Coble and Brophy (1994) have suggested that changes in  $S$  may be due to the direct biological production of compounds such as proteins, amino acids, and carbohydrates, which absorb more strongly in the UV range than in the visible, and possible diurnal cycling of UV-absorbing compounds. Data from Vernet and Whitehead (1996) support this suggestion that phytoplankton exudates can influence CDOM absorbance characteristics at least on a short timescale.

In the present experiment, the steepening of  $S$  was positively correlated ( $r = 0.7$ ,  $p < 0.01$ ) with Chl  $a$  concentration, whereas no such covariance was observed with bacterial abundance. However, the steepening of  $S$  was also positively correlated with the absorbed radiation dose ( $r = 0.85$ ,  $p < 0.01$ ). Gao and Zepp (1998) demonstrated that the LMW < 1 kDa fraction separated by ultrafiltration had a different wavelength dependence for rates of photobleaching

than the unfractionated parent material. This may be relevant in the mesocosms considering that the majority of DOM released by phytoplankton is likely to be of low molecular weight,  $MW < 1$  kDa (Jensen 1983; Lancelot 1984; Ridal and Moore 1993). Gao and Zepp's study indicates that photobleaching of the LMW fraction under full-spectrum light is slower in the UVB wavelength range than the UVA range. These results imply that a shift toward lower molecular weight DOM could change the wavelength dependence of photobleaching such that further photobleaching would result in increased  $S$ .

The results from the current study might be equally well explained by solely considering the kinetics of photobleaching in optically thick systems. In contrast to optically thin systems where half-lives are independent of concentrations, the half-life of  $a_{\text{CDOM}}$  in optically thick systems is dependent on initial concentration (Zepp and Cline 1977). Therefore, half-lives decrease with increasing wavelength due to lower initial absorbances and despite the slower photobleaching rates. For example, the average half-life for  $a_{\text{CDOM}}$  at 280 nm for the four systems was 36.4 d, whereas the average half-life at 450 nm was only 13.5 d. Consequently, photobleaching as observed in the mesocosms would yield an increase in  $S$  with time. However, both initial  $a_{\text{CDOM}}$  and photobleaching rates may have been influenced by biological activity. Thus, based on the current results, it is impossible to determine the relative importance of biological (phytoplankton or bacterial) production of absorbing moieties versus the photochemical reactivity of DOM on the changes in  $S$ . Nevertheless, during the experiment, there was an evolution of  $a_{\text{CDOM}}$  spectral characteristics demonstrating that transformation and/or replacement of CDOM through in situ processes can alter  $S$ , and mixing of waters with different CDOM pools need not be involved.

Changes in  $a_{\text{CDOM}}$  are the net result of the difference in production processes and removal processes. The measured decreases in  $a_{\text{CDOM}}$  demonstrate that over the course of the experiment the production rates were slower than the removal rates. Although the production and removal processes may both depend on biological or photochemical activity, the strong correlation of CDOM absorbance loss with radiation dose and the lack of correlation with bacterial abundance suggests that the primary removal mechanism in the mesocosm was photochemically mediated. Earlier studies using monochromatic light sources have shown that the maximum loss in CDOM absorbance occurs in the region of the wavelength of irradiation, but smaller absorbance losses at other wavelengths occur concurrently (Kouassi and Zika 1992). Gao and Zepp (1998) hypothesized that photobleaching was the result of both direct photoreactions of CDOM and secondary reactions involving active oxygen species. Rate data from these two investigations showed faster absorbance loss at short wavelengths than at longer wavelengths for unfractionated CDOM under full-spectrum irradiation. In principle, these results imply that +UVB treatments in the present work should have had more photobleaching than NAT treatments, especially at UVB wavelengths where the added radiation from the lamps was the greatest. The mesocosm results are somewhat contrary to this presumption.

In the fast mixing regime,  $a_{\text{CDOM}}$  losses and photobleaching rates (versus total Ein absorbed) in the NAT light system were nearly identical to the +UVB light system. Although the UVA, UVB, and total absorbed doses in both mixing systems were slightly higher in the +UVB treatment, the only significant differences were for the absorbed UVB dose (ANOVA  $p < 0.01$ ). Examination of the rates shown in Fig. 5D, however, reveals that the response to total UVB-absorbed dose was on average 1.9 times less in the +UVB fast system than in the NAT fast system. In the slow systems, the +UVB light treatment had an average 1.7-fold decrease in response compared to the +UVB treatment. A reduction in response to UVB radiation in photobleaching in association with the increased UVB radiation provided by the lamps is perplexing. It suggests that there may be a mechanism or mechanisms by which the photobleaching effects of the added UVB were mitigated, such as the stimulation of CDOM production. In other words, without a light influence on CDOM production,  $a_{\text{CDOM}}$  loss per absorbed UVB photon should have been relatively equal within each of the mixing treatments due to the similarities of other measured parameters. This would have then produced larger absolute losses of absorbance in the +UVB systems compared to the NAT systems, which was not seen in the fast systems.

One possible mechanism for a reduction of photobleaching response to increased UVB is photoreactions that yield more strongly absorbing products from weakly absorbing reactants. Kieber et al. (1997) have proposed photo-oxidation of triglycerides and fatty acids as an integral part of the humification of algal-derived DOM. They showed that the photo-induced humification of fatty acids added to sterile seawater resulted in a postirradiation increase in absorbance. Although full sunlight incubations were used and a wavelength dependence was not given by Kieber and coworkers, a UVB influence on the process could in part explain the patterns seen in the mesocosms. Indeed, Wheeler (1972) has shown that UV irradiation, 290 to 450 nm of sterile seawater containing linoleic acid, linolenic acid, or a phytoplankton lipid extract consistently resulted in increased UV absorbances, which indicates that the photochemical reaction products absorbed UV radiation more intensely than their precursors. Recent work has suggested that enhanced UVB can promote production of some fatty acids by phytoplankton (Wängberg et al. 1999). However, the results were not consistent and may be related to the species present or the nutrient status of the exposed cells (Goes et al. 1994). Either an increase in released fatty acids with increased UVB exposure or a UVB-driven humification reaction could act to retard photobleaching rates under enhanced UVB.

Another possibility for a UVB-induced effect resulting in increased UV absorbance is the production of photoprotective pigments or other compounds by plankton that subsequently become incorporated into the CDOM pool (Vernet and Whitehead 1996). Microsporine-like amino acids (MSAAs) have been proposed as photoprotective compounds produced by phytoplankton under UVB stress (Karentz 1994). Release of these compounds, which absorb strongly in the UV range, into the DOM pool could alter  $a_{\text{CDOM}}$  values. However, MSAAs measured in phytoplankton from random samples during the experiment were very low

to nondetectable (Roy pers. comm.). Although it seems unlikely, based on these random samples, that MSAs were released in large enough quantities to have an influence on CDOM absorption, Vernet and Whitehead (1996) indicated that the accumulation of MSAs in the DOM pool was not a simple function of intracellular concentrations. The reported molar extinction coefficients for these compounds are very large (28,100 to 44,700 liter mole<sup>-1</sup> cm<sup>-1</sup>) in the UV region. Based on these molar extinction coefficients and absorption spectra, absorbance due to MSA concentrations in the nanomolar range should be detectable with the spectrophotometer used in the current study and would contribute almost exclusively to absorbance in the UV range.

In contrast with the fast systems, the slow mixing systems appeared more consistent with previous filtered-water degradation studies. With slower mixing and lower concentrations of plankton-derived products, photoreactions in the +UVB slow light treatment yielded higher absorbance losses and faster photobleaching rates (versus total Ein absorbed) than the NAT slow system at the wavelengths below 315 nm (Fig. 5A). This would be expected based on previous results showing faster photobleaching rates of unfractionated DOM at UVB wavelengths (Gao and Zepp 1998) and the augmentation of UVB provided by the lamps. However, examination of Fig. 4 shows that the rate constant at a specific UVB wavelength per Ein absorbed at that wavelength is smaller in the +UVB slow system than the NAT slow system. This indicates lower photobleaching quantum efficiency for UVB photons in the +UVB light treatment and that the degree of photobleaching was not directly proportional to the increase in UVB. In effect, although the slow systems behaved more like a filtered-water sample, the influence of biological activity and its consequences on photoreactions were not totally eliminated. Furthermore, the influence of mixing (discussed below) tended to retard photobleaching in the slow systems and its influence would also tend to yield less photohumification reactions if these reactions mainly involved UVB or short UVA light.

Although the seemingly equivocal photobleaching results in response to enhanced UVB in the present study are probably due to both changes in CDOM optical properties and photoreactivity resulting from biological activity of the systems, they do not control it completely. In fact, the results clearly show that the rate of photobleaching is faster than the rate of any photo-induced humification or replacement of destroyed chromophores by new plankton-derived ones. This implies that physical factors influencing the photobleaching reactions can outweigh biological influences. Comparison of the two mixing regimes also gives some insight into physical influences. The same general pattern of photobleaching was seen for both mixing regimes, which argues in favor of comparable biological inputs to the photobleaching process. Thus, if biological processes were the primary factor controlling photobleaching, then the slow systems should have shown greater photobleaching due to the smaller input of plankton-derived DOM. Accordingly, the two slow light treatments should have behaved more like filtered-water studies. An argument has been made for the latter case (discussed earlier); however, overall the slow systems had slower photobleaching rates and lower losses than

the fast systems. This behavior is consistent with views on the role of mixing in aquatic photochemistry. Studies such as those by Plane et al. (1987) and Doney et al. (1995) have shown that mixing rates can exert a strong influence on the rates and distribution of photoprocesses in the water column. In general, lack of or slower mixing confines photoreactions to the very top of the water column in water bodies where there is strong light attenuation of wavelengths involved in the photoreactions and the rates of these primary photoreactions decrease exponentially with depth (Plane et al. 1987). With more thorough mixing, fresh photochemical reactants are continually added to the photoactive layer, which results in higher rates of photolysis for the entire water column (Hedlund and Youngson 1972). In the mesocosms, the depth of 1% UVB radiation was ~1 m, or about half the depth of the water column, and less than 1.5 m for the shorter wavelengths of UVA (Fig. 1C). As such, the lower half of our water columns was essentially devoid of primary photoreactions resulting from UVB wavelengths and about 50% of UVA wavelengths. On the other hand, 19% of near-surface PAR was still present at the maximum depth of 2.25 m. Thus, the water flow rates through the upper 1 m should have a direct influence only on the photochemical processes depending on UV radiation.

Primary photochemical reaction rates are directly proportional to the rate of light absorption only in completely mixed, optically thin water bodies or where the reactant is the sole absorber (Zepp and Cline 1977). In optically thick water columns with competition amongst chromophores for photons, differences in mixing rates can affect photochemical reaction rates. The differences in turnover due to the mixing regimes dictates that the volume passing through the upper 1 m, approximately the UV photoactive layer, in the fast systems be approximately 3 times greater than the slow systems. The faster turnover would tend to limit the extent of CDOM self-shading and increase photoreaction rates. In contrast, longer wavelengths in PAR were present to the maximum depth of the mesocosms, and therefore flow through the upper 1 m would be less important. In effect, the faster turnover acts to produce a photoactive layer that appears deeper than it actually is and the influence should be greatest at shorter wavelengths where the attenuation with depth is the fastest and self-shading is the greatest. The slower photobleaching in the slow systems at all wavelengths combined with the measured wavelength dependence of light attenuation indicates that the majority of all photobleaching, even that extending into PAR, originates from light absorbed in the UVB and short UVA wavelength ranges.

There are many difficulties in extrapolating from laboratory-based photochemical studies to natural aquatic systems. In particular, rates of absorption by reactants depend on accurate predictions of in situ light penetration into the water column, which are complicated in the presence of plankton and other suspended particulate matter. Previous suggestions that increases in UVB due to stratospheric ozone loss would produce more photobleaching at UVB wavelengths and subsequently deeper penetration of UVB appear to oversimplify the interactions of these biotic and abiotic influences on photoprocesses in the water column. Although the mesocosm results clearly indicate a major role of UVB radiation in

CDOM photobleaching, the enhancement of UVB did not result in a proportional increase in photobleaching. The results here indicate that concurrent biological activity can modify, but apparently not prevent, the photobleaching process. Thus, in situ photobleaching may not only depend on incident light characteristics, but also on concurrent biological activity. In addition, mixing processes will play an important role in determining the magnitude of CDOM absorbance loss. The results also suggest that photo-induced transformations in the presence of recently produced DOM may cause the CDOM spectral slope to increase. Consequently, the ratios of UVB to UVA and PAR would be reduced following photobleaching, although penetration of all wavelengths would increase. Although photodegradation of apparently refractory DOM has been shown to stimulate bacterial activity, recent observations suggest that DOM pools that include freshly released DOM may be rendered less bioavailable. Despite the fact that bacterial abundance decreased in the mesocosms, the systems are too complex to justifiably argue photochemical processes as the principal cause. Nevertheless, the mesocosm results may be a further indication of a dual role for photochemical processes in oceanic DOM cycling such that some labile plankton byproducts are incorporated into the CDOM pool while more refractory material is altered to enhance bioavailability.

## References

- BAKER, K. S., AND R. C. SMITH. 1982. Bio-optical classification and model of natural waters. 2. *Limnol. Oceanogr.* **27**: 500–509.
- BELZILE, C., AND OTHERS. 1998. An experimental tool for the study of the effects of ultraviolet radiation on planktonic communities: A mesocosm approach. *Environ. Technol.* **19**: 667–682.
- BENNER, R., AND B. BIDDANDA. 1998. Photochemical transformation of surface and deep marine dissolved matter: Effects of bacterial growth. *Limnol. Oceanogr.* **43**: 1373–1378.
- , AND M. STROM. 1993. A critical review of the analytical blank associated with DOC measurements by high-temperature catalytic oxidation. *Mar. Chem.* **41**: 153–160.
- BIDDANDA, B., AND R. BENNER. 1997. Carbon, nitrogen, and carbohydrate fluxes during the production of particulate and dissolved organic matter by marine phytoplankton. *Limnol. Oceanogr.* **42**: 506–518.
- BLOUGH, N. V., O. C. ZAFIRIOU, AND J. BONILLA. 1993. Optical absorption spectra of waters from the Orinoco River Outflow: Terrestrial input of colored organic matter to the Caribbean. *J. Geophys. Res.* **98**: 2271–2278.
- , AND R. G. ZEPP. 1995. Reactive oxygen species in natural waters, p. 280–333. *In* C. S. Foote, J. S. Valentine, A. Greenberg, and J. F. Liebman [eds.], *Active oxygen in chemistry*. Chapman and Hall.
- BOOTH, C., AND OTHERS. 1997. Impacts of solar UVR on aquatic microorganisms. *Photochem. Photobiol.* **65**: 252–269.
- BRICAUD, A., A. MOREL, AND L. PRIEUR. 1981. Absorption by dissolved organic matter of the sea (yellow substance) in the UV and visible domains. *Limnol. Oceanogr.* **27**: 43–53.
- BROPHY, J., AND D. CARLSON. 1989. Production of biologically refractory dissolved organic carbon by natural seawater microbial populations. *Deep-Sea Res.* **36**: 497–507.
- BROWN, M. 1977. Transmission spectroscopy examinations of natural waters. *Estuar. Coast. Mar. Sci.* **5**: 309–317.
- CARDER, K., R. STEWARD, G. HARVEY, AND P. ORTNER. 1989. Marine humic and fulvic acids: Their effects on remote sensing of ocean chlorophyll. *Limnol. Oceanogr.* **34**: 68–81.
- CARLSON, C., H. DUCKLOW, D. HANSELL, AND W. SMITH. 1998. Organic carbon partitioning during spring phytoplankton blooms in the Ross Sea polynya and the Sargasso Sea. *Limnol. Oceanogr.* **43**: 375–386.
- COBLE, P., AND M. BROPHY. 1994. Investigation of the geochemistry of dissolved organic matter in coastal waters using optical properties. *SPIE—Ocean Optics XII* **2258**: 377–389.
- DEGRANDPRE, M. D., A. VODACEK, R. K. NELSON, E. J. BRUCE, AND N. V. BLOUGH. 1996. Seasonal seawater optical properties of the U.S. Middle Atlantic Bight. *J. Geophys. Res.* **101**: 22727–22736.
- DONEY, S. C., R. G. NAJJAR, AND S. STEWART. 1995. Photochemistry, mixing and diurnal cycles in the upper ocean. *J. Mar. Res.* **53**: 341–369.
- GAO, H., AND R. G. ZEPP. 1998. Factors influencing photoreactions of dissolved organic matter in a coastal river of the southeastern United States. *Environ. Sci. Technol.* **32**: 2940–2946.
- GOES, J., N. HANDA, S. TAGUCHI, AND T. HAMA. 1994. Effect of UV-B radiation on the fatty acid composition of the marine phytoplankton *Tetraselmis* sp.: Relationship to cellular pigments. *Mar. Ecol. Prog. Ser.* **114**: 259–274.
- GORDON, H. 1989. Can the Lambert-Beer law be applied to the diffuse attenuation coefficient of ocean water? *Limnol. Oceanogr.* **34**: 1389–1409.
- GREEN, S. A., AND N. V. BLOUGH. 1994. Optical absorption and fluorescence properties of chromophoric dissolved organic matter in natural waters. *Limnol. Oceanogr.* **39**: 1903–1916.
- GUO, L., AND P. SANTSCHI. 1997. Isotopic and elemental characterization of colloidal organic matter from the Chesapeake Bay and Galveston Bay. *Mar. Chem.* **59**: 1–15.
- HARVEY, G., D. BORAN, L. CHESAL, AND J. TOKAR. 1983. The structure of marine humic and fulvic acids. *Mar. Chem.* **12**: 119–132.
- HEDGES, J. I. 1992. Global biogeochemical cycles: Progress and problems. *Mar. Chem.* **39**: 67–93.
- , R. KEIL, AND R. BENNER. 1997. What happens to terrestrially-derived organic matter in the sea? *Org. Geochem.* **27**: 195–212.
- HEDLUND, R., AND C. YOUNGSON. 1972. The rates of photodecomposition of Picloram in aqueous systems, p. 159–172. *In* S. Faust [ed.], *Fate of organic pesticides in the aquatic environment*. American Chemical Society.
- JENSEN, L. 1983. Phytoplankton release of extracellular organic carbon, molecular weight composition, and bacterial assimilation. *Mar. Ecol. Prog. Ser.* **11**: 39–48.
- KARENTZ, D. 1994. Ultraviolet tolerance mechanisms in Antarctic marine organisms, p. 93–110. *In* C. S. Weiler and P. A. Penhale [eds.], *Ultraviolet radiation in Antarctica: Measurements and biological effects*. American Geophysical Union.
- KEIL, R., AND D. KIRCHMAN. 1994. Abiotic transformation of labile protein to refractory protein in sea water. *Mar. Chem.* **45**: 187–196.
- KIEBER, D. J., J. A. MCDANIEL, AND K. MOPPER. 1989. Photochemical source of biological substrates in seawater: Implications for geochemical carbon cycling. *Nature* **341**: 637–639.
- KIEBER, R., L. HYDRO, AND P. SEATON. 1997. Photooxidation of triglycerides and fatty acids in seawater: Implication toward the formation of marine humic substances. *Limnol. Oceanogr.* **42**: 1454–1462.
- , X. ZHOU, AND K. MOPPER. 1990. Formation of carbonyl compounds from UV-induced photodegradation of humic substances in natural waters: Fate of riverine carbon in the sea. *Limnol. Oceanogr.* **35**: 1503–1515.

- KIRK, J. T. O. 1994. Light and photosynthesis in aquatic ecosystems, 2nd ed. Cambridge Univ. Press.
- , AND OTHERS. 1994. Measurements of UV-B radiation in two freshwater lakes: An instrument comparison. *Arch. Hydrobiol. Beih. Ergeb. Limnol.* **43**: 71–99.
- KOUASSI, A. M., AND R. G. ZIKA. 1992. Light-induced destruction of the absorbance property of dissolved organic matter in seawater. *Toxicol. Environ. Chem.* **35**: 195–211.
- KUHN, P., H. BROWMAN., B. MCARTHUR, AND J.-F. ST-PIERRE. 1999. Penetration of ultraviolet radiation in the waters of the estuary and Gulf of St. Lawrence. *Limnol. Oceanogr.* **44**: 710–716.
- LANCELOT, C. 1984. Extracellular release of small and large molecules by phytoplankton in the southern bight of the North Sea. *Estuar. Coast. Shelf Sci.* **18**: 65–77.
- LAROCHE, P. 1998. SeaWIFS validation program in the St. Lawrence estuary and Gulf. Fifth International Conference on Remote Sensing for Marine and Coastal Environments.
- LEVASSEUR, M., J.-C. THERRIAULT, AND L. LEGENDRE. 1984. Hierarchical control of phytoplankton succession by physical factors. *Mar. Ecol. Prog. Ser.* **19**: 211–222.
- MALCOLM, R. 1990. The uniqueness of humic substances in each of soil, stream and marine environments. *Anal. Chim. Acta* **232**: 19–30.
- MILLER, W. L. 1998. Effects of UV radiation on aquatic humus: Photochemical principles and experimental considerations. *Ecol. Stud.* **133**: 125–143.
- . 1994. Recent advances in the photochemistry of natural dissolved organic matter, p. 111–128. *In* G. R. Helz, R. G. Zepp, and D. G. Crosby [eds.], *Aquatic and surface photochemistry*. Lewis.
- , AND R. G. ZEPP. 1995. Photochemical production of dissolved inorganic carbon from terrestrial organic matter: Significance to the oceanic carbon cycle. *Geophys. Res. Lett.* **22**: 417–420.
- MONFORT, P., AND B. BALEUX. 1992. Comparison of flow cytometry and epifluorescence microscopy for counting bacteria in aquatic ecosystems. *Cytometry* **13**: 188–192.
- MOPPER, K., Z. FENG, S. B. BENTJEN, AND R. F. CHEN. 1996. Effects of cross-flow filtration on the absorption and fluorescence properties of seawater. *Mar. Chem.* **55**: 53–74.
- , X. ZHOU, R. J. KIEBER, D. J. KIEBER, R. J. SIKORSKI, AND R. D. JONES. 1991. Photochemical degradation of dissolved organic carbon and its impact on the oceanic carbon cycle. *Nature* **353**: 60–62.
- MORAN, M. A., AND R. G. ZEPP. 1997. Role of photoreactions in the formation of biologically labile compounds from dissolved organic matter. *Limnol. Oceanogr.* **42**: 1307–1316.
- MORRIS, D. P., AND B. R. HARGREAVES. 1997. The role of photochemical degradation of dissolved organic carbon in regulating the UV transparency of three lakes on the Pocono Plateau. *Limnol. Oceanogr.* **42**: 239–249.
- NAGANUMA, T., S. KONISHI, T. INOUE, T. NAKANE, AND S. SUKIZAKI. 1996. Photodegradation or photoalteration? Microbial assay of the effect of UV-B on dissolved organic matter. *Mar. Ecol. Prog. Ser.* **135**: 309–310.
- NELSON, J. R., AND S. GUARDA. 1995. Particulate and dissolved spectral absorption on the continental shelf of the southeastern United States. *J. Geophys. Res.* **100**: 8715–8732.
- NELSON, N., D. SIEGEL, AND A. MICHAELS. 1998. Seasonal dynamics of colored dissolved material in the Sargasso Sea. *Deep-Sea Res. I* **45**: 931–957.
- NIEKE, B., R. REUTER, R. HEUERMANN, H. WANG, M. BABIN, AND J. C. THERRIAULT. 1997. Light absorption and fluorescence properties of chromophoric dissolved organic matter (CDOM) in the St. Lawrence Estuary. *Cont. Shelf Res.* **17**: 235–252.
- OBERNOSTERER, I., B. REITNER, AND G. HERNDL. 1999. Contrasting effects of solar radiation on dissolved organic matter and its bioavailability to marine bacterioplankton. *Limnol. Oceanogr.* **44**: 1645–1654.
- PAGES, J., AND F. GADEL. 1990. Dissolved organic matter and UV absorption in a tropical hyperhaline estuary. *Sci. Total Environ.* **99**: 173–204.
- PARSONS, T., Y. MAITA, AND C. LALLI. 1984. A manual of chemical and biological methods for the analysis of seawater. Pergamon.
- PLANE, J. M. C., R. G. ZIKA, R. G. ZEPP, AND L. A. BURNS. 1987. Photochemical modeling applied to natural waters, p. 250–267. *In* R. G. Zika and W. J. Cooper [eds.], *Photochemistry of environmental aquatic systems*. American Chemical Society.
- PORTER, K., AND Y. FEIG. 1980. The use of DAPI for identifying and counting aquatic microflora. *Limnol. Oceanogr.* **25**: 943–948.
- RIDAL, J., AND R. MOORE. 1993. Resistance to UV and persulphate oxidation of dissolved organic carbon produced by selected marine phytoplankton. *Mar. Chem.* **42**: 167–188.
- ROCHELLE-NEWALL, E., T. FISHER, C. FAN, AND P. GLIBERT. 1999. Dynamics of chromophoric dissolved organic matter and dissolved organic carbon in experimental mesocosms. *Int. J. Remote Sens.* **20**: 627–641.
- STROMM, S., R. BENNER, S. ZIEGLER, AND M. DAGG. 1997. Planktonic grazers are a potentially important source of marine dissolved organic carbon. *Limnol. Oceanogr.* **42**: 1364–1374.
- VALENTINE, R. L., AND R. G. ZEPP. 1993. Formation of carbon monoxide from the photodegradation of terrestrial organic carbon in natural waters. *Environ. Sci. Technol.* **27**: 409–412.
- VERNET, M., AND K. WHITEHEAD. 1996. Release of ultraviolet-absorbing compounds by the re-tide dinoflagellate *Lingulodinium polyedra*. *Mar. Biol.* **127**: 35–44.
- VODACEK, A., N. V. BLOUGH, M. D. DEGRANDPRE, E. T. PELTZER, AND R. K. NELSON. 1997. Seasonal variation of CDOM and DOC in the Middle Atlantic Bight: Terrestrial inputs and photooxidation. *Limnol. Oceanogr.* **42**: 674–686.
- WÄNGBERG, S.-Å., K. GARDE, K. GUSTAVON, AND J.-S. SELMER. 1999. Effects of UVB radiation on marine phytoplankton communities. *J. Plankton Res.* **21**: 147–166.
- WHEELER, J. 1972. Some effects of solar levels of ultraviolet radiation on lipids in artificial sea water. *J. Geophys. Res.* **77**: 5302–5306.
- WILLIAMSON, C. E., R. S. STEMBERGER, D. P. MORRIS, T. M. FROST, AND S. G. PAULSEN. 1996. Ultraviolet radiation in North American lakes: Attenuation estimates from DOC measurements and implications for plankton communities. *Limnol. Oceanogr.* **41**: 1024–1034.
- ZAFIRIOU, O. C., J. J. DUBIEN, R. G. ZEPP, AND R. G. ZIKA. 1984. Photochemistry of natural waters. *Environ. Sci. Technol.* **18**: 358A–371A.
- ZEPP, R. G., T. V. CALLAGHAN, AND D. J. ERICKSON. 1995. Effects of increased solar ultraviolet radiation on biogeochemical cycles. *Ambio* **24**: 181–187.
- , AND D. M. CLINE. 1977. Rates of direct photolysis in aquatic environment. *Environ. Sci. Technol.* **11**: 359–366.

Received: 22 June 1999

Accepted: 15 November 1999

Amended: 22 November 1999